Formation of *n*-Alkane Layers at the Vapor/Water Interface

Oh-Sun Kwon,[†,§] Huaiyu Jing,[†] Kwanwoo Shin,*[,†] Xiaohui Wang,[‡] and Sushil K. Satija*[,‡]

Department of Chemistry and Program of Integrated Biotechnology, Sogang University, Shinsoo, Mapogu, Seoul 121-742, Korea, and National Institute of Standards and Technology, 100 Bureau Drive, Gaithersburg, Maryland 20899

Received July 12, 2007. In Final Form: September 15, 2007

We present a study on the initial wetting behaviors of two low molecular weight alkanes, heptane and octane, at the vapor/water interface using both neutron and X-ray reflectometry. Combined X-ray and neutron reflectivity studies data showed that a uniform film, which has never been reported, was formed continuously at 25 °C. As the adsorptive deposition continued, each adsorbed film was saturated at a specific equilibrium thickness: 48 and 36 Å for deuterated heptane and octane, respectively, and 21 Å for hydrogenated octane. The thickness of the adsorbed layer measured by neutron reflectivity is in agreement with that measured using X-ray reflectivity. Our observations of continuous and saturated adsorption behaviors are analyzed qualitatively using a kinetic adsorption model.

Introduction

Layer formation of normal alkanes (denoted as *n*-alkanes, C_nH_{2n+2}) on water is related to a number of fundamental physical phenomena, such as intermolecular dispersion force and wetting theories,[1−5] as well as applications for oil recovery[6] and liquid lens.[7]

It has long been postulated that the free energy of interactions between vapor/alkane and alkane/water (i.e., disjoining pressure) should be balanced by favorable or unfavorable long-range van der Waals interactions,[5] depending on the sign of the Hamaker constant,[8] to form a stable wetting layer on water. Although it is well known that the shorter *n*-alkanes, in general, favor the complete wetting state while the incomplete wetting state (partial wetting) occurs with an increase in the number of carbon atoms in the *n*-alkane molecules, the question of wetting phenomena related to the specific chain size of *n*-alkanes has not yet been answered.[4] In addition, many results during the past decade have shown that the alkane/water system is far from simple and yields even conflicting evidence: as examples, Del Cerro et al. found that the *n*-alkanes with $n > 5$ did not spread on the water surface,[9] while Hauxwell et al.[10] and Richmond et al.[11] reported the formation of wetting layers of *n*-alkanes with $5 \leq n < 8$. Pethica argued later that Hauxwell et al. might have had inadequate vapor pressure in their systems, which caused unreliable measurements and uncertainties in their results.[12]

Under the variation of thermodynamic conditions, a variety of wetting transitions of *n*-alkanes, such as a critical (continuous) wetting,[3,12−16] a first-order (discontinuous) wetting,[17] and a sequence of two wetting,[18] have been found mostly using optical ellipsometry.[4] Some interesting phenomena in wetting transitions, for example, irreversible hysteresis[19] and surface crystallization of high *n*-alkanes at above solidification temperature,[20] have been observed. The results of the wetting transition measurements are also still controversial and not yet fully understood, although the existence of a third wetting state, that is, a pseudo-partial wetting state, explains some wetting phase transitions satisfactorily.[6]

A partial wetting layer and a submonolayer film of octane at $T = 25$ °C were suggested theoretically in the global wetting phase diagram[17] and were observed by ellipsometry measurements.[4] However, ambiguity in the interpretation of density and thickness, when the layer is ultrathin, was mentioned in the same paper. Yet, there was no report verifying the layer structure of octane by any other experimental tools. Although neutron and X-ray reflectometry are powerful tools for the investigation of ultrathin films due to its high spatial resolution perpendicular to the surface, very few papers using these scattering techniques[21] have addressed the alkane/water interfacial systems, including these wetting phenomena. Therefore, we performed in situ X-ray and neutron reflectivity measurements to crosscheck the initial

* Corresponding authors. (K.S.) Tel.: 82-2-705-8441. Fax: 82-2-701-0967. E-mail: kwshin@sogang.ac.kr. (S.K.S.) Tel.: (301) 975-5250. E-mail: sushil.satija@nist.gov.

† Sogang University.

‡ National Institute of Standards and Technology.

§ Present address: Anyang University, Seoul, Korea.

(1) Charvolin, J.; Joanny, J. F. In *Liquids at Interfaces*; Zinn-Justin, J., Ed.; North-Holland: Amsterdam, 1990; Vol. 48.

(2) Dietrich, S. In *Phase Transitions and Critical Phenomena*; Domb, C., Lebowitz, J. L., Eds.; Academic Press: London, 1988; Vol. 12.

(3) Akatsuka, S.; Yoshigiwa, H.; Mori, Y. H. *J. Colloid Interface Sci.* **1995**, *172*, 335.

(4) Pfohl, T.; Möhwarld, H.; Riegler, H. *Langmuir* **1998**, *14*, 5285.

(5) Hirasaki, G. J. In *Contact Angle, Wettability and Adhesion*; Mittal, K. E., Ed.; Utrecht: London, 1993.

(6) Bertrand, E.; Bonn, D.; Broseta, D.; Dobbs, H.; Indekeu, J. O.; Meunier, J.; Ragil, K.; Shahidzadeh, N. *J. Petrol. Sci. Eng.* **2002**, *33*, 217.

(7) Kuiper, S.; Hendriks, B. H. W. *Appl. Phys. Lett.* **2004**, *85*, 1128.

(8) Hamaker, H. C. *Physica* **1937**, *4*, 1058.

(9) Cerro, C. D.; Jameson, G. J. *J. Colloid Interface Sci.* **1980**, *78*, 362.

(10) Hauxwell, F.; Ottewill, R. H. *J. Colloid Interface Sci.* **1970**, *34*, 473.

(11) Richmond, P.; Ninham, B. W.; Ottewill, R. H. *J. Colloid Interface Sci.* **1973**, *45*, 69.

(12) (a) Pethica, B. A. *Langmuir* **1996**, *12*, 5851. (b) Lou, A.; Pethica, B. A. *Langmuir* **1997**, *13*, 4933.

(13) (a) Cahn, J. W. *J. Chem. Phys.* **1977**, *66*, 3667. (b) Cahn, J. W.; Hilliard, J. E. *J. Chem. Phys.* **1958**, *28*, 258.

(14) Pfohl, T.; Riegler, H. *Phys. Rev. Lett.* **1999**, *82*, 783.

(15) Ragil, K.; Meunier, J.; Broseta, D.; Indekeu, J. O.; Bonn, D. *Phys. Rev. Lett.* **1996**, *77*, 1532.

(16) (a) Ross, D.; Bonn, D.; Meunier, J. *Nature* **1999**, *400*, 737. (b) Ross, D.; Bonn, D.; Meunier, J. *J. Chem. Phys.* **2001**, *114*, 2784.

(17) Bertrand, E.; Dobbs, H.; Broseta, D.; Indekeu, J. O.; Bonn, D.; Meunier, J. *Phys. Rev. Lett.* **2000**, *85*, 1282.

(18) (a) Shahidzadeh, N.; Bonn, D.; Ragil, K.; Broseta, D.; Meunier, J. *Phys. Rev. Lett.* **1998**, *80*, 3992. (b) Weiss, V. C.; Indekeu, J. O. *Fluid Phase Equilib.* **2004**, *222*, 269.

(19) Bonn, D.; Kellay, H.; Wegdam, G. H. *Phys. Rev. Lett.* **1992**, *69*, 1975.

(20) Wu, X. Z.; Sirota, E. B.; Sinha, S. K.; Ocko, B. M.; Deutsch, M. *Phys. Rev. Lett.* **1993**, *70*, 958.

(21) (a) Lee, L. T.; Langevin, D.; Farnoux, B. *Phys. Rev. Lett.* **1991**, *67*, 2678. (b) Esibov, L.; Sarkisov, D.; Jeng, U.-S.; Crow, M. L.; Steyerl, A. *Physica B* **1998**, 241.

10.1021/la702084e CCC: $37.00
Published on Web 10/23/2007

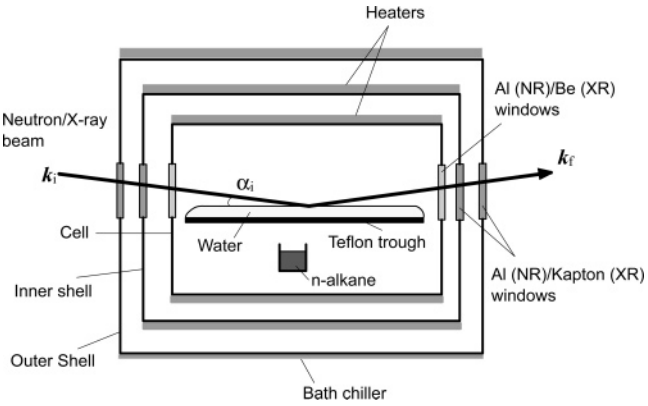

Figure 1. Experimental setup for neutron and X-ray reflectivity measurements: it consists of one cell inside two shells. The cell contains a water bath and an *n*-alkane reservoir. Thickness of an alkane layer on the vapor/water interface was measured by neutron and X-ray reflectivity, separately, as a function of the scattering vector, $\mathbf{q} = \mathbf{k}_f - \mathbf{k}_i$, where $\mathbf{k}_i$ ($\mathbf{k}_f$) is the incident (scattered) wavevector. For specular reflection, $q_z = (4\pi/\lambda) \sin \alpha_i$, where α_i is the angle of incidence and *z*-direction is normal to the interface.

adsorbed structures of *n*-alkanes on a nanometer scale. In this Article, thus, we present a combined study of neutron reflectivity (NR) and X-ray reflectivity (XR) to investigate adsorbed layers of two low *n*-alkanes, heptane and octane, at the vapor/water interface at 25 °C. After careful week-long measurements, we found that the alkanes layers were formed as uniform layers, which were never observed previously. We confirmed that these two reflectivity data produced identical results. Using these two complementary methods, consequently, we found positive evidence that these two alkanes form thermodynamically stable wetting layers at the vapor/water interface at room temperature.

Experimental Details

Deuterated (>99%) octane (*d*-C_8, M_w = 132.4 g/mol), heptane (*d*-C_7, M_w = 116.2 g/mol), and hydrogenated octane (*h*-C_8, M_w = 114.2 g/mol) purchased from Cambridge Isotope Laboratory were used. To ensure a chemically pure alkane, we carefully followed a published purification procedure, by passing an alkane through a 10 cm high LC column, at least three times with basic alumina (pH 10.0).[22] Highly pure water (resistivity = 18.0 MΩ cm) purified by a Millipore Milli-QUV Plus system was used for the subphase. To check the long-term stability of an immiscible alkane/water interface, the interfacial tension of a bulk system was monitored separately using the Wilhelmy plate technique. The measured variation for octane was $|\Delta\gamma| < 0.15$ mN/m during 24 h, which proved that the interface was free from any surface active impurities. Purified water was poured on a Teflon mini-trough (14 cm × 7 cm), which had been rigorously cleaned with chloroform. A sample of *n*-alkane in a small Pyrex dish was placed near the water trough in a cell with the volume of about 0.6 dm^3, as shown in Figure 1. The sample was filled with the volume of about 10 mL, which was enough to be evaporated into the saturated vapors in the closed cell. The vapors moved diffusively, and some proportion of them arriving near the water surface would be adsorbed on the surface.

Figure 1 shows a schematic view of the experimental setup for the measurements of NR and XR. The lids, with their thin aluminum windows, were positioned to transmit the incident and reflected neutron beams, while they were substituted with beryllium and Kapton windows for the XR measurements. The tight sealing between the lids and cell and shells was achieved using indium O-rings. Special care was taken to ensure temperature stability. First, the trough and an alkane were kept in a cylindrical thermostated aluminum canister (cell, inner shell, and outer shell) as shown in the figure. Two superstable thermistors (YSI 46046, resistance 10.0 kΩ at T = 25.00 °C) mounted immediately above and below the cell were used to maintain the same temperature. The temperatures of the cell and inner shell were then independently controlled via two temperature controllers (Lakeshore LS340). While the cell temperature was maintained at $T = 25.00 \pm 0.005$ °C, the inner shell was set to be $T = 24.90 \pm 0.01$ °C. The inner shell was then inserted into the copper coiled outer shell, whose temperature was set to be $T = 24.00 \pm 0.01$ °C, just below the temperature of the inner shell, and was controlled by a water chiller. The outer shell was insulated by a 3 cm thick polyurethane form from the ambient temperature ~23 °C. With this temperature gradient system, the inner shell was kept within a variance of temperature $|\Delta T| < 0.01$ °C, and the temperature fluctuation across the sample was in the range of 0.005 °C over the entire experimental period. The whole chamber was placed on an active vibration isolation platform (Herzan TS-15 for X-ray reflectometer and Herzan AVI-350 for neutron reflectometer).

NR was performed at the National Institute of Standards and Technology (NIST, Gaithersburg, MD) using the NG7 horizontal reflectometer (λ = 4.76 Å). A one-dimensional position sensitive detector (PSD), which has 255 channels oriented perpendicular to the sample surface, enables the simultaneous recording of both specular intensity and background scattering. The reflected intensity was obtained by integrating the peak channels. An angular difference of ± 0.156° from the specular peak, where the flat incoherent background scattering is shown, was chosen to obtain the background intensity ($<1 \times 10^{-6}$ counts/s), and then the background was subtracted from the reflected intensity. The measured intensity was then converted to the absolute reflectivity, via normalization with the detector/monitor ratio below the critical angle where total external reflection occurs.

XR was performed using a D8 Advance (Bruker, Germany) with a vertical goniometer, which allows the study of a liquid surface, without moving a sample during measurements. A ceramic anode X-ray generator was used to produce Cu Kα radiation (λ = 1.542 Å), followed by a paralleling of the incident beam with a Göbel mirror (GM III). Two slits defined the incident beam size and reduced the vertical divergence. For the smallest reflection angle, the vertical slit gaps were typically 20 μm, corresponding to a vertical divergence of 0.07°, while the horizontal slits were widely opened. A scintillator detector was followed by a slit with a vertical gap of 0.6 mm.

For specular reflection, the scattering vector, $\mathbf{q} = \mathbf{k}_f - \mathbf{k}_i$, is only in the *z*-direction, which is normal to the interface. Because $q_x = q_y = 0$, it is given by $q_z = (4\pi/\lambda) \sin \alpha_i$, where α_i is the angle of incidence as shown in Figure 1. By the Born approximation at $q_z > q_c$, where q_c is the critical angle for total reflection, the reflectivity, $R(q_z)$, is expressed essentially as:

$$R(q_z) \propto R_F \left| \int dz \, \frac{d\rho(z)}{dz} \exp(-iq_z z) \right|^2 \quad (1)$$

where R_F is the Fresnel reflectivity at an infinitely sharp interface and $\rho(z)$ is the neutron (electron density for X-ray) scattering length density (SLD). Thus, by reflectivity measurement it is possible to detect even a very small variation of an adsorbed alkane, which induces the SLD gradient to the *z*-direction. For NR, the SLD gradient at the vapor/water interface is extremely small, because the SLD of H_2O is negative, $\rho = \sum b_i n_i = -5.6 \times 10^{-7}$ Å^{-2}, where b_i is the scattering length and n_i is the number density of atomic species i. For this reason, deuterated alkanes are used to maximize the contrast of reflection from alkane interfaces. This contrast method is possible due to the difference of the scattering length of the isotopes of hydrogen, that is, $b_H = -3.74 \times 10^{-5}$ Å and $b_D = 6.67 \times 10^{-5}$ Å.

For a single thin layer with two rough interfaces, eq 1 can be modified to

$$R(q_z) = \frac{R_F}{\rho_2^2} [(\rho_1 - \rho_2) \exp(-q_{z1} q_{z2} \sigma_2^2) + \rho_1 \exp(-q_{z0} q_{z1} \sigma_1^2)]^2 \exp(iq_z d) \quad (2)$$

(22) Mitrinovic, D. M.; Tikhonov, A. M.; Li, M.; Huang, Z.; Schlossman, M. L. *Phys. Rev. Lett.* **2000**, *85*, 582.

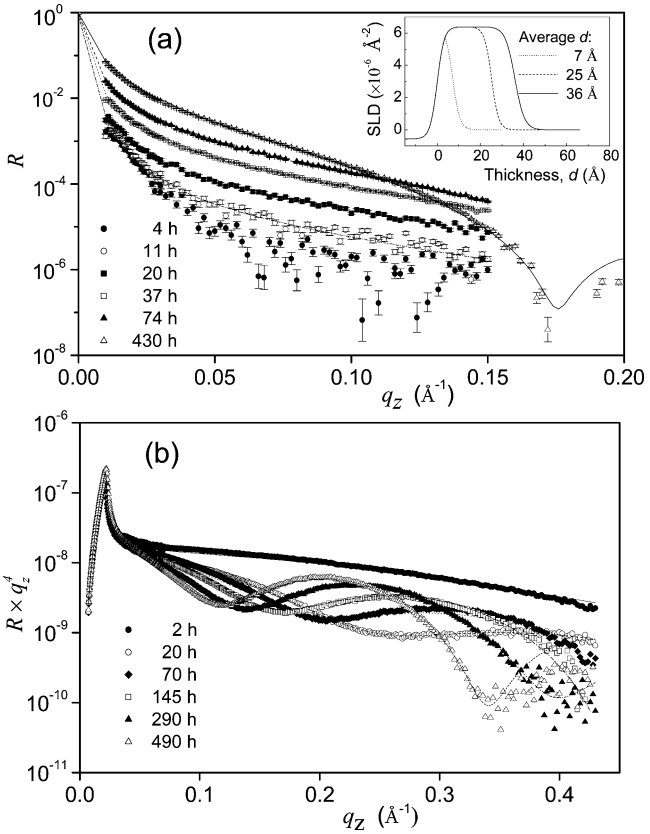

Figure 2. (a) The neutron reflectivity versus the scattering vector q_z for d-C_8 at 25 °C with respect to six different adsorption times. The reflectivity increment in time is gradually slowed down and saturated at $t \approx 400$ h. (inset) Lines represent SLD's corresponding to $t = 11$ h (• • •), 74 h (- - -), and 430 h (—). (b) The X-ray reflectivity data for the same sample. Curved lines represent the best fit.

where ρ is the *SLD*, σ is the root-mean-square roughness, and d is the layer thickness with the subscripts 0, 1, and 2 denoting air, alkane, and water, respectively. Thus, two surface roughnesses of vapor/alkane and alkane/water interfaces are taken into account in the damping factor. The exact thickness of the single layer can be obtained from the oscillation period in oscillating factor, Δq_z, as $d = 2\pi/\Delta q_z$.

We repeatedly scanned the reflectivity to monitor the thickness and the density changes of alkanes adsorbed on the vapor/water interface as a function of time. To analyze the reflectivity data, the recursive Parratt formalism was used.[23] The sharp interfaces are smeared by rms roughness, σ, which is given by convoluting the infinitely sharp profile with a Gaussian smoothing function. We systematically varied and then optimized the fitting parameters SLD, d, and σ until χ^2 was minimized.

Results and Discussion

Figure 2a shows the NR measurement data for the adsorbed layer of d-C_8 as a function of q_z at six different adsorption times. All fits to the reflectivity data (lines) in Figure 2a were performed initially with a single-layer model as shown in the inset. The first scattering intensity after sealing the cell (●) at $t = 4$ h is close to the Fresnel reflectivity of H_2O surface (not shown), indicating that the adsorbed amount is negligible. The reflection intensity increases progressively as the contrast at the interface between air and water subphase is being modified due to accumulation of adsorbed d-C_8 molecules. A minimum, which originates from a coherent interference of reflected beams, is clearly shown in the NR spectrum at $t = 430$ h, implying a formation of a macroscopic octane layer with relatively sharp interfaces. It appears at $q_z \approx 0.18$ Å^{-1}, and we obtain an about 36 Å thick d-C_8 layer with roughnesses of about 5 and 6 Å for octane/water and vapor/octane interfaces, respectively. Until $t = 430$ h, the first minimum from reflectivity oscillations was, however, not observed for the maximum q_z-range of 0.01−0.20 Å^{-1} in the present experiment. Without the first minimum from reflectivity oscillations, it is difficult to extract the exact thickness. Because the reflection intensity is proportional to SLD, which is a combined value of the scattering lengths of the constituent nuclei, $\sum b_i$, and the thickness of the octane layer, d, a fitted value of thickness can be induced by the other fitting parameters of the octane. For example, a discontinuous (island-like) or a pseudo-partial wetting state[6] requires a surface density from the low surface coverage with very rough interfacial lengths, or a two-layer model, respectively[24] (Supporting Information). The single-layer model used for the reflectivity spectra for $t \leq 430$ h was based on the assumption that the continuous accumulation had occurred. Because the frequency of oscillations in a reflectivity spectrum corresponds inversely to the layer thickness, a thickness less than 31 Å or less could be expected when $t \leq 430$ h. If a uniform thin layer <31 Å has been formed, in contrast to the previous reports,[4,17] then the first minimum in reflectivity oscillation should be observed at $q_z > 0.2$ Å^{-1}.

To extract the exact thicknesses for $t < 430$ h without the prior assumption for a uniform layer model used in the above NR analysis, XR measurements at the same conditions were performed. The XR significantly extends the maximum q_z-range up to 0.5 Å^{-1}; therefore, the first minimum from the layers with $d \leq 12$ Å will appear in its wide range of reflectivity spectrum if our model is correct. The specular XR curves obtained from d-C_8 at different adsorption times are shown in Figure 2b. Note that the measured reflectivities, R, and their fits were normalized by the respective q_z^{-4}, to highlight the unique interference fringes, which contain only the damping factors due to the surface roughnesses, and an oscillating term due to the uniform film thickness without q_z^{-4} decay contained R_F in eq 2. The figure demonstrates that the first fringe appeared at $q_z \approx 0.25$ Å^{-1} when $t = 22$ h, indicating that a 17 Å thick homogeneous thin layer was formed. This layer is exactly consistent with the layer thickness obtained from the fit to NR spectrum with the model of a single uniform layer. Because XR detects the variation of the electron density $\rho_{el}(z)$ in the direction normal to the surface, averaged in the parallel plane to the sample surface, note that the layer thicknesses, d, the density contrasts and the interfacial roughnesses, σ_1 and σ_2, defined by the probability density, were used for the fitting parameters. Depending on $\rho_{el}(z)$, the index of refraction of d-C_8 layer is sufficiently different from that of the water subphase. In this case, neglecting absorption, at an incident energy of 8 keV, the calculated index of refraction $n = 1 - \delta$ with dispersion δ of d-C_8 is $n(d\text{-}C_8) = 1 - 2.850 \times 10^{-6}$. The δ is given by the electron density, that is, $\delta = \lambda^2 \rho_{el} r_o / 2\pi$, where r_o is the classical electron radius.

To retrieve detailed information on d and σ, we assumed that the d-C_8 film has the same density as the bulk liquid (0.815 g/cm^3) and used the interfacial roughness, $\sigma_2 = 5.5$ Å, at the octane/water interface, which was published by Schlossman and co-workers using X-ray reflectometry.[22] In general, the fits shown as lines matched the experimental curves quite well. The two variable fitting parameters produced thickness and vapor/octane roughness, σ_1. For simple liquids, the roughness was shown to be dominated by the thermally induced capillary wave ampli-

(23) Ankner, J. F.; Majkrzak, C. F.; Satija, S. K. *J. Res. Natl. Inst. Stand. Technol.* **1993**, *98*, 47.

(24) Russell, T. P. *Mater. Sci. Rep.* **1990**, *5*, 171.

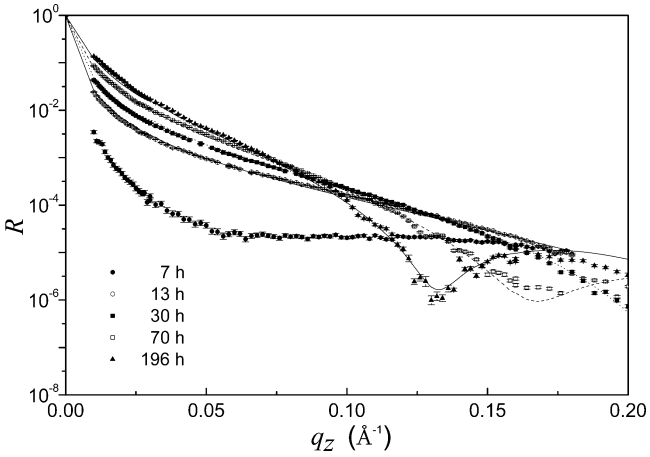

Figure 3. The neutron reflectivity versus the scattering vector q_z for *d*-C_7 at 25 °C with respect to five different adsorption times. Curved lines represent the best fits.

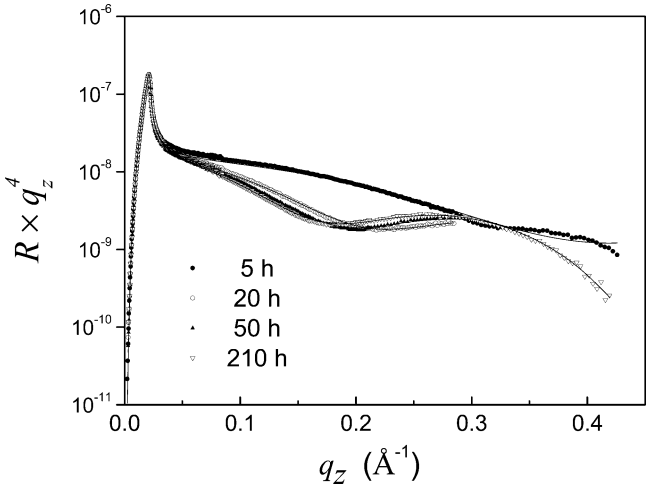

Figure 4. The X-ray reflectivity versus the scattering vector q_z for *h*-C_8 at 25 °C with respect to five different adsorption times. Curved lines represent the best fits.

tudes,[25] which are inversely proportional to $\gamma^{1/2}$, where γ is the surface tension. Provided that $\gamma(H_2O) = 72.0$ mN/m, γ(*n*-octane) = 21.1 mN/m, and the measured water surface roughness, we calculated $\sigma_1 = \sigma(H_2O)(\gamma(H_2O)/\gamma(n\text{-octane}))^{1/2} \approx 5.9$ Å, in good agreement with the fitted value.[26] It should be noted that the reflectivity profiles were changing rapidly with time in the first 20 h, indicating the growing of the octane film on water surface immediately after closing the chamber. Therefore, a slight discrepancy between the measured (●) and fitted spectrum for $t = 2$ h is probably due to kinetic changes in the octane layer. After the initial fast adsorption, the reflectivity profile changed slowly but progressively, before it reached the equilibrium state, which did not change at least in $t = 490$ h during the measurements.

As *t* increases (from 70 to 490 h), one can see that the amplitude of the beating rapidly decreases and the frequency of the Kiessig fringes becomes more visible to the second minimum of q_z. Thus, in contrast to the previous report,[14] the observed fringes in the XR spectra suggest that a smooth octane layer has been formed, which is also in good agreement with the NR results above.

Further specular NR curves were measured for deuterated heptane, *d*-C_7, at the vapor/water interface; the results are shown in Figure 3. A single minimum appears at $t \geq 70$ h, which moves progressively to lower q_z at longer adsorption times. The film grows much faster than the octane film does before it reaches 40 Å. The growing rate becomes less sharp at $t \geq 100$ h. Essentially, the adsorption kinetics is similar to the *d*-C_8 case whose equilibrium thickness is 36 Å. The equilibrium thickness of *d*-C_7 is 48 Å. Again, a single layer model for *d*-C_7 provided a good fit over the entire range of reflectivity spectra.

Now, we need to discuss the rather surprising observations in the reflectivity results, indicative of the presence of a smooth layer of octane with a saturation thickness at the vapor/water interface. Pfohl et al.[4] reported that hexane and heptane wet the air/water interface with an ultrathin film of molecular thickness that is topped with droplets of micrometer dimensions, whereas octane adsorbed only in a submonolayer film under ambient condition in their 13 h-long measurements using an ellipsometric technique. Therefore, their submonolayer status may not be at equilibrium, because the 36 Å thick layer of *d*-C_8 appeared only after 400 h (~17 days!) of equilibrium time in our system. There are two possible reasons for the discrepancy: (a) the adsorption process is extremely slow so that Pfohl and his co-workers simply could not observe the equilibrium stage of the adsorption; or (b) the isotope effect of octane due to the deuteration alters the nature of principal interactions, where the van der Waals forces and the spreading coefficient are balanced.

We point out here that none of the experiments previously had measured long enough to observe such a slow process. Furthermore, for the ellipsometry technique,[4] they used Drude's formula to convert the measured ellipticity into the film thickness, which made the interpretation of the ellipticity rather difficult for films of only a few decades angstroms in thickness. The ellipsometry technique has an advantage in the short scanning time of milliseconds for one scan and a spatial footprint of a few millimeters in diameter. Besides, the advantages of neutron and X-ray scattering techniques are the larger footprints (>50 mm × 150 mm), and fringes are used for direct thickness conversion, which should clearly be more beneficial in our experimental system.

To rule out the possibility of an isotope effect as pointed out in the above item (b), we measured the adsorption of hydrogenated octane (*h*-C_8) by XR, as the results are shown in Figure 4. In contrast to the 36 Å thick layer for *d*-C_8, the thickness of *h*-C_8 reaches about 21 Å with a dispersion δ of 2.462×10^{-6} because $n(h\text{-}C_8) = 1 - 2.462 \times 10^{-6}$. Nevertheless, the existence of macroscopic thin layers of *d*-C_8 and *h*-C_8 was confirmed on the water surface. However, their behaviors were very different. After about 40 h, *h*-C_8 reached a stable film at 21 Å, while the *d*-C_8 film grew fast before it reached 20 Å, followed by slow growth from 20 Å to somewhere around 36 Å. Although the reason for this discrepancy is peculiar and not clearly understood so far, it is probably due to a subtle difference in the Hamaker constant or purity difference (99.999% for *h*-C_8 and 99.9% for *d*-C_8). The best fitted thickness variations as a function of adsorption time for all measurements have been plotted in Figure 5.

Now, we further discuss the second observation of continuous layer formation of those alkanes. Two models of the adsorption kinetics of alkane molecules on a water surface, so-called wetting transitions, have been suggested so far as mentioned in the previous section: (a) a continuous wetting type, where there is the wetting phase transition from a partial to a complete state; and (b) a discontinuous wetting type, in which the transition has a pseudo-partial wetting state in which a thin film coexists with

(25) Sanyal, M. K.; Sinha, S. K.; Huang, K. G.; Ocko, B. M. *Phys. Rev. Lett.* **1991**, *66*, 628.

(26) Lide, D. R. *CRC Handbook of Chemistry and Physics*; CRC Press: Boca Raton, FL, 2001.

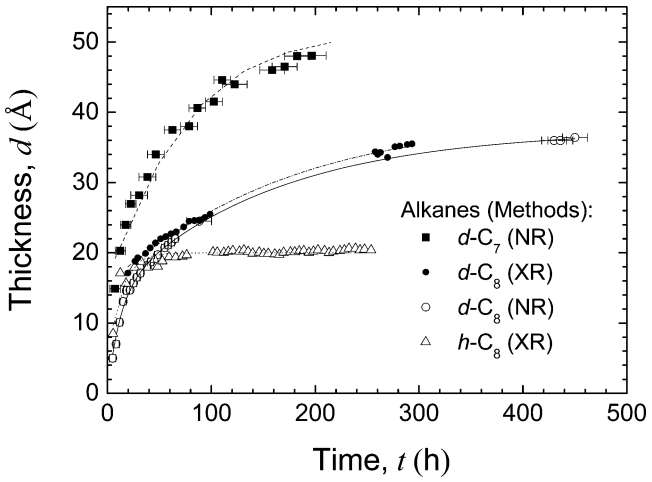

Figure 5. Variation of thickness for various *n*-alkanes as a function of adsorption time. Curved lines represent the best fits.

residual droplets[21] when the temperature or vapor pressure is changed. Despite various uncertainties involved in fitting our reflectivity data, all of the fitted thicknesses for three samples (Figures 2−4) appear as a smooth logarithmically increasing trend without any noticeable deviations. Thus, we may conclude that our result indicates that the film formation is similar to a sequence of complete wetting transitions under the condition of increasing alkane volumes at the vapor/water interface at the constant temperature.

This similarity in the adsorption process indicates that a kinetic model can be applied (see Supporting Information). Plateaus or inflections in surface coverage as a function of adsorption time are usually interpreted in terms of an equilibrium state in the adsorption kinetics. Thus, we can infer that the alkane layer has passed through at least two different states involving the following steps. Initially, there is a progressive rise in thickness, corresponding to the preferred adsorption state that the water surface attracts the alkane molecules as mass diffusion of alkane vapors occurs, until a layer several times the alkane's radius of gyration is built up. Subsequently, the kinetic adsorption process of the layer formation (for *d*-C_8, *h*-C_8, and *d*-C_7) steadily reduces and a steady state of the alkane film is maintained, indicative of an adsorption process and saturation due to equilibrium. This kinetic transition from fast to slow adsorption can be explained qualitatively by the assumption that the property of adsorptive interaction at the transition is changed. Thus, we can separate the origins of adsorptive intermolecular interactions into the adhesive force between polar water molecules and nonpolar hydrophobic alkane vapors at initial adsorption time and the cohesive force between alkane vapors and condensed alkanes, which are already adsorbed on the water interface after transition. They must, therefore, have different affinitive or strength properties. In addition, such a difference incorporates with both short and long-range dispersion forces. Consequently, we can conclude that the slow adsorption after transition is mainly induced by the weaker long-range dispersion force. However, although such a qualitative kinetic description seems to be plausible to interpret this equilibrium layer formation including the saturated phenomenon, there are still many obstacles to applying the mathematical kinetic formalism,[27] which was applied to a liquid adsorption.

Conclusions

Using neutron and X-ray reflectometry, the formation of films of two low carbon chain *n*-alkanes, heptane and octane, at the interface between water and a mixture of air and alkane vapors has been studied at a fixed temperature. The measured reflectivity data clearly showed that each alkane formed a continuous wetting layer. It is remarkable that two different reflectivity measurements showed similar results. The fact that octane and heptane formed uniform layers on a pure water surface is quite surprising, because it has been reported many times that they do not wet pure water. It should be emphasized that our results suggest that they show the complete wetting states at room temperature under the condition of increasing their volumes. More work, however, is required to understand the wetting transition phenomena under different variation of thermodynamic properties, such as temperature and pressure, and surfactant impurity for many practical applications.

Acknowledgment. We thank Dr. Albert Steyerl of the University of Rhode Island and Dr. Benjamin Ocko of BNL for a fruitful discussion. This work was supported by a grant from the "Center for Nanostructured Materials Technology" under the "21st Century Frontier R&D Program", the KAIST-BAERI of Korea, and US DOE under contract no. DE-FG02-91ER45445.

Supporting Information Available: Fitting models and fits (a discontinuous wetting type, a discontinuous wetting type with a thin film coexisting with residual droplets, and continuous). This material is available free of charge via the Internet at http://pub.acs.org.

LA702084E

(27) (a) Hubbard, J. B.; Silin, V.; Plant, A. L. *Biophys. Chem.* **1998**, *75*, 163. (b) Zheng, Z.; Stroumpoulis, D.; Parra, A.; Petzold, L.; Tirrell, M. *J. Chem. Phys.* **2006**, *124*, 064904.